Localisation of WE-14 Immunoreactivity in the Developing Mouse Limbo-Corneal Nerve Net

WILLIAM JAMES CURRY,* SIMON BROCKBANK, ANNA PATRICIA MCCOLLUM, CLIONA BOYLE, AND DAVID GIBSON
Centre of Ophthalmology and Vision Science, The Queen's University of Belfast, BT12 6BA, North Ireland, United Kingdom

KEY WORDS   immunocytochemistry; neuropeptide; neuronal

ABSTRACT   WE-14 is generated in subpopulations of chromogranin A immunopositive endocrine cells and neurons including those innervating the anterior uvea. This study investigated WE-14 in intact sclero-limbo-corneal tissue from embryonic (E17), neonatal (N0-N16), and adult mice using immunocytochemistry and confocal scanning laser microscopy. Weak WE-14 immunostaining was observed at birth in nerve fibre tracts entering the corneal mid-stroma from the limbo-scleral junction. Immunopositive fibre tracts were evident throughout the cornea at N3; by N5 the mid-stromal plexus had begun to generate fibre populations extending toward the developing corneal epithelium, and some varicose fibres terminated amongst the developing epithelium. Immunostaining was evident at N7 in the developing limbo-scleral nerve net and some fibres exhibited a close association with unidentified vascular elements. By N11 and in subsequent neonates, the cornea had developed a distinct stratified nerve net composed of thick mid-stromal and thinner upper stromal nerve fibre bundles; both possessed populations of varicose WE-14 immunopositive fibres. In the adult, a sub-epithelial network of varicose WE-14 immunopositive fibres were evident at the limbo-scleral junction. Some fibres exhibited a close association with unidentified vascular elements, while others extended into the upper peripheral corneal stroma. WE-14 was evident in leashes throughout the basal corneal epithelium and generated fibres ramifying between the stratified epithelium with some fibres terminating amongst the outermost corneal epithelia. This study has demonstrated that WE-14 was evident in the limbo-corneal nerve net at birth and that its detection parallels corneal development to adulthood, where WE-14 is evident in a subpopulation of nerve fibres. *Microsc. Res. Tech. 62:408–414, 2003.*   © 2003 Wiley-Liss, Inc.

INTRODUCTION

The cornea forms the transparent dome at the front of the eye; it covers the iris, pupil, and anterior chamber and provides most of an eye's optical power. It is one of the most highly innervated external tissues in the body, possessing both sensory and autonomic innervation. Anatomical studies have revealed that the density and pattern of corneal innervation is species dependent (Zander and Weddell, 1951). A small number of sensory nerves contain the catecholamine synthesising enzyme tyrosine hydroxylase (Ueda et al., 1989), whilst a major population contains an array of neuropeptides; substance P (SP) (Miller et al., 1981), calcitonin gene-related peptide (CGRP) (Stone et al., 1988a), galanin (Stone et al 1988b), and pituitary adenylate cyclase-activating peptide (PACAP) (Moller et al., 1993). Cornea sympathetic innervation contains the classical neurotransmitters noradrenaline and serotonin, and neuropeptide Y (NPY) (Marfurt, 2000). Corneal parasympathetic innervation, which appears limited, contains vasoactive intestinal polypeptide (VIP), met-enkephalin, and NPY (Jones and Marfurt, 1998). Additional neuropeptides and pan-neuronal markers detected include cholecystokinin (CCK) (Palkama et al., 1986), vasopressin (Too et al., 1989), brain natriuretic peptide (Yamamoto et al., 1991), neurotensin (Tinsley et al., 1988), neurone-specific enolase (NSE) (Ueda et al., 1989), and protein gene product (PGP) 9.5 (Marfurt et al., 1993) have been detected in corneal nerves.

Chromogranin A (CgA) is an established neuroendocrine marker; it is a member of the granin family of acidic glycoproteins that are localised to dense cored secretory granules in endocrine and neuronal cells (Helle, 2000). Since its discovery, CgA has been credited with multiple physiological roles including granulogenesis (Gorr et al. 1989), modulation of intragranular calcium (Reiffen and Gratzl 1986), cell adhesion (Gasparri et al. 1997), and CgA peptide fragments have been reported to exhibit antibacterial and antifungal properties (Lugardon et al., 2000). The cloning and sequencing of CgA molecules revealed multiple pairs of conserved basic residues that flank homologous peptide domains (Hutton et al., 1988); these features are characteristic of prohormones. The identification of the CgA-derived peptides, vasostatin (Aardal and Helle, 1992), pancreastatin (PST) (Tatemoto et al., 1986), WE-14 (Conlon et al., 1992; Curry et al., 1992), catostatin (Mahata et al., 1997), and GE-25 (Kirchmair et al.,

*Correspondence to: Dr. W.J. Curry, Centre of Ophthalmology & Vision Science, Institute of Clinical Science, Queen's University, Grosvenor Road, Belfast, BT12 6BA, N Ireland, UK. E-mail: j.w.curry@qub.ac.uk
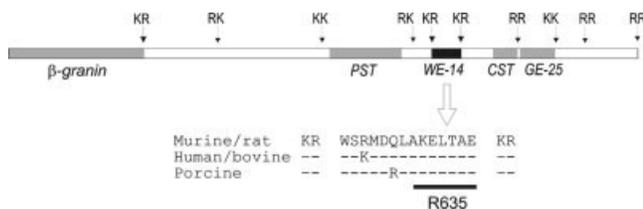
Fig. 1. Diagrammatic representation of murine and rat chromogranin A with the conserved pairs of basic residues above the location of the derived peptides B-granin, pancreastatin (PST), catostatin (CST), GE-25, and WE-14 with its single letter amino acid sequence and inter-species homology, the C-terminal hexapeptide antigen (line), and antibody code (R635).

1994) further supports this biological role (Fig. 1). WE-14 is flanked by pairs of conserved basic residues and exhibits a high degree of inter-species homology. It is generated in a subpopulation of adult rat neuroendocrine cells (Curry et al., 1991) and to varying degrees in human neuroendocrine neoplasia (Gleeson et al., 1996; Heaney et al., 2000). Developmental studies have shown that WE-14 is generated at an early stage of endocrine gland generation in the rat and pig (Barkatullah et al., 1997, 2001) and that it has an ancient lineage (Curry et al., 2002).

Studies have detected CgA in retinal neurons (Gibson and Munzo, 1993; Nolan et al. 1985) and a previous study has revealed WE-14 is present in porcine retinal cell populations and neurones innervating the anterior uvea (Curry et al., 2003). This study employed a well-characterised WE-14 antiserum to investigate its distribution in foetal, neonatal, and adult mouse sclero-limbo-corneal tissues (Fig. 1).

MATERIALS AND METHODS

Embryonic (E17), neonatal (N0-N16), and adult (6 weeks old) C57 mice housed under standard laboratory conditions (12:12 hour light-dark; fed and watered ad libitum) were killed by CO_2 asphyxiation. Intact E17 heads and dissected corneo-scleral preparations (N0-adult) were immersion fixed in buffered 4% (w/v) paraformaldehyde (PFA) in 0.1 M phosphate buffered saline (PBS) pH 7.2 (4 hours, 4°C). Intact E17 heads (n = 4) were laterally bisected and intact corneo-scleral specimens (n = 4 per age; N0-adult) were placed in incubation buffer (0.1 M PBS containing 0.3% (v/v) Triton X100, 0.3% (w/v) bovine serum albumin, and 0.1% (w/v) sodium azide) for 48 hours, followed by preincubation with non-immune goat serum (1:100, 24 hours) in incubation buffer and washed (18 hours) with incubation buffer. The tissues were incubated (1:200, 48 hours, 4°C) with a C-terminal specific WE-14 antiserum (R635) (Curry et al. 1991) (Fig. 1); washed in incubation buffer (48 hours), incubated with porcine anti-rabbit (FITC) secondary antiserum (1:200, 48 hours) (DAKO, Denmark) and washed (48 hours) in incubation buffer. Intact tissue specimens were incubated with propidium iodide (5 μg/ml; 30 minutes) followed by multiple washes for 24 hours with incubation buffer. All protocols were performed at 4°C with constant gentle agitation in a dark chamber. Maltese cross corneo-scleral specimens were prepared prior to mounting in 90% (v/v) glycerol in 0.1 M PBS containing

anti-fade reagent (1,4-diazobicyclo(2,2,2)octane). Specimens were viewed using a Bio-Rad microradiance confocal scanning laser microscope. Immunocytochemical control studies were performed using 4% (w/v) PFA fixed cryoprotected adult tissue sections (30 μm). This included the liquid phase preabsorption of the WE-14 antiserum with synthetic human WE-14 and the C-terminal hexapeptide antigen (Y°KELTAE) as described previously (Barkatullah et al. 1997, 2001; Norlen et al., 2001) and replacement of the primary antiserum with non-immune rabbit serum and the omission of the fluorescein isothiocynate tagged swine anti-rabbit sera. Unless otherwise stated, all chemicals were purchased from Sigma Chemical Company, Poole, UK.

RESULTS

WE-14 immunostaining was detected in nerve fibres of the developing and adult mouse limbo-corneal nerve net (Figs. 2–4). Immunocytochemical control studies demonstrated that WE-14 immunostaining was abolished by preincubation of the C-terminal serum with both the specific antigen (Y°KELTAE; 3.5 nM) and human WE-14 (1 nM). No immunostaining was observed following the inclusion of non-immune rabbit serum and with the omission of the porcine anti-rabbit FITC.

No WE-14 immunostaining was observed in the cornea in situ within intact eyes of bisected head tissue at E17. All subsequent observations were generated following confocal scanning laser microscopic (CLSM) analysis of whole mount corneo-scleral tissues. At N0/1, diffuse weak to moderate WE-14 immunostaining was observed in a population of peripheral nerve fibre bundles entering from the limbo-scleral junction of the developing cornea in a mid-stromal zone (Fig. 2a). At N3, moderately intense WE-14 immunoreactivity was detected in large mid-stromal nerve fibre bundles extending from the limbo-corneal junction toward the central cornea (Fig. 2b). By N5, nerve fibre tracts derived from the mid-stromal plexus extended toward the developing corneal epithelium, terminating in varicose fibres within the basal zone of the corneal epithelia (Fig. 2c). A similar pattern of WE-14 immunostaining was observed in the developing cornea at N7; however, additional WE-14 immunoreactivity was observed in a rudimentary scleral-limbo-corneal nerve net (Fig. 2d). At N11, the cornea had developed a distinct stratified nerve net comparable to that of the adult. This was composed of a network of thick mid-stromal nerve tracts (Fig. 2e) that gave rise to an upper stromal nerve net composed of fine nerve tracts that extended into the developing corneal epithelium; all these nerve tracts possessed populations of varicose WE-14 immunopositive fibres. By N16 WE-14, immunostaining was observed in an extensive ramifying varicose fibre network beneath the limbo-corneal epithelium. Some fibres exhibited a close association with unidentified superficial limbal vessels that encircled the corneal (Fig. 2f). The pattern and intensity of WE-14 immunostaining in limbo-corneal nerves at N16 was comparable to that observed in adult mouse (Fig. 3a).

CSLM analysis of adult limbo-corneal preparations revealed the extent of WE-14 immunostaining (Figs.
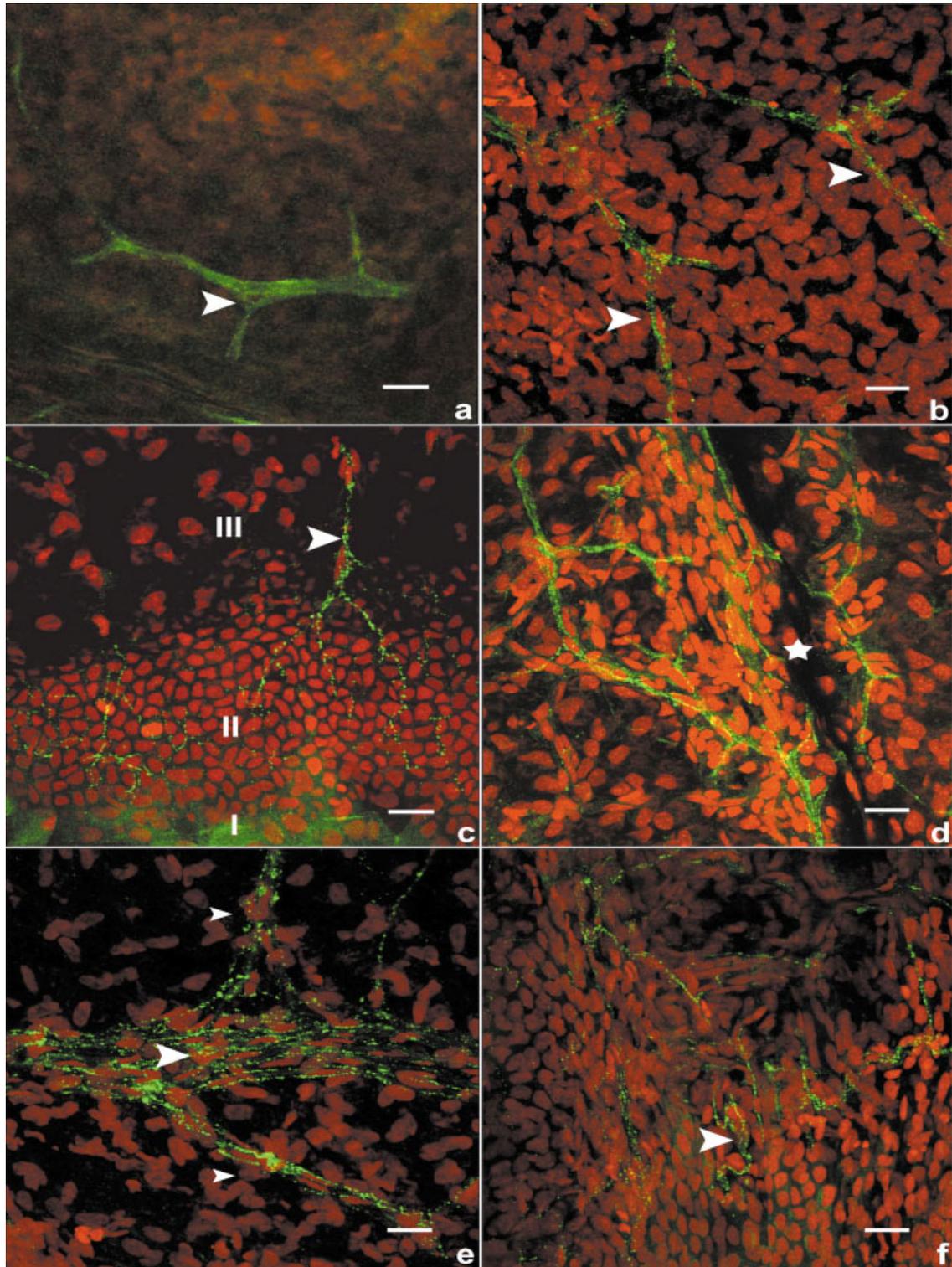
Fig. 2. Confocal scanning laser microscope Z-series images of WE-14 immunostaining in whole-mount preparation of the developing mouse limbo-corneal nerve net (green) with propidium iodide nuclear counter stain (red) (a–f). Each image represents a composite CSLM Z series image generated from the following total section thickness: a, 65.1; b, 46.6; c, 22.2; d, 26.0; e, 6.1; f, 12.8 μm, respectively. Weak diffuse immunostaining in nerve fibre tracts enters the cornea from the limbo-scleral junction (arrowhead) at N0 (**a**). Moderately intense varicose immunostaining in mid-stromal fibres in the developing central cornea at N3 (arrowhead) (**b**). Intense immunostaining in thin nerve fibre tracts (arrowhead) entering the basal epithelial cells (III); these fibres bifurcate to generate varicose fibres that ramify amongst the basal layer of the developing corneal epithelium (II) and terminate amongst superficial epithelial cells (I) at N5 (**c**). Intense neuronal WE-14 immunostaining in the developing sub epithelial limbo-corneal nerve (star) net at N7 (**d**). Characteristic intense varicose WE-14 immunostaining of fibres within a prominent mid-stromal nerve fibre tract (arrowhead) (**e**) and in individual nerve fibres in close association with unidentified sub epithelial limbal vessels (arrowhead) at N11 (**f**). Scale bar = 20 μm. [Color figure can be viewed in the online issue, which is available at www.interscience.wiley.com.]
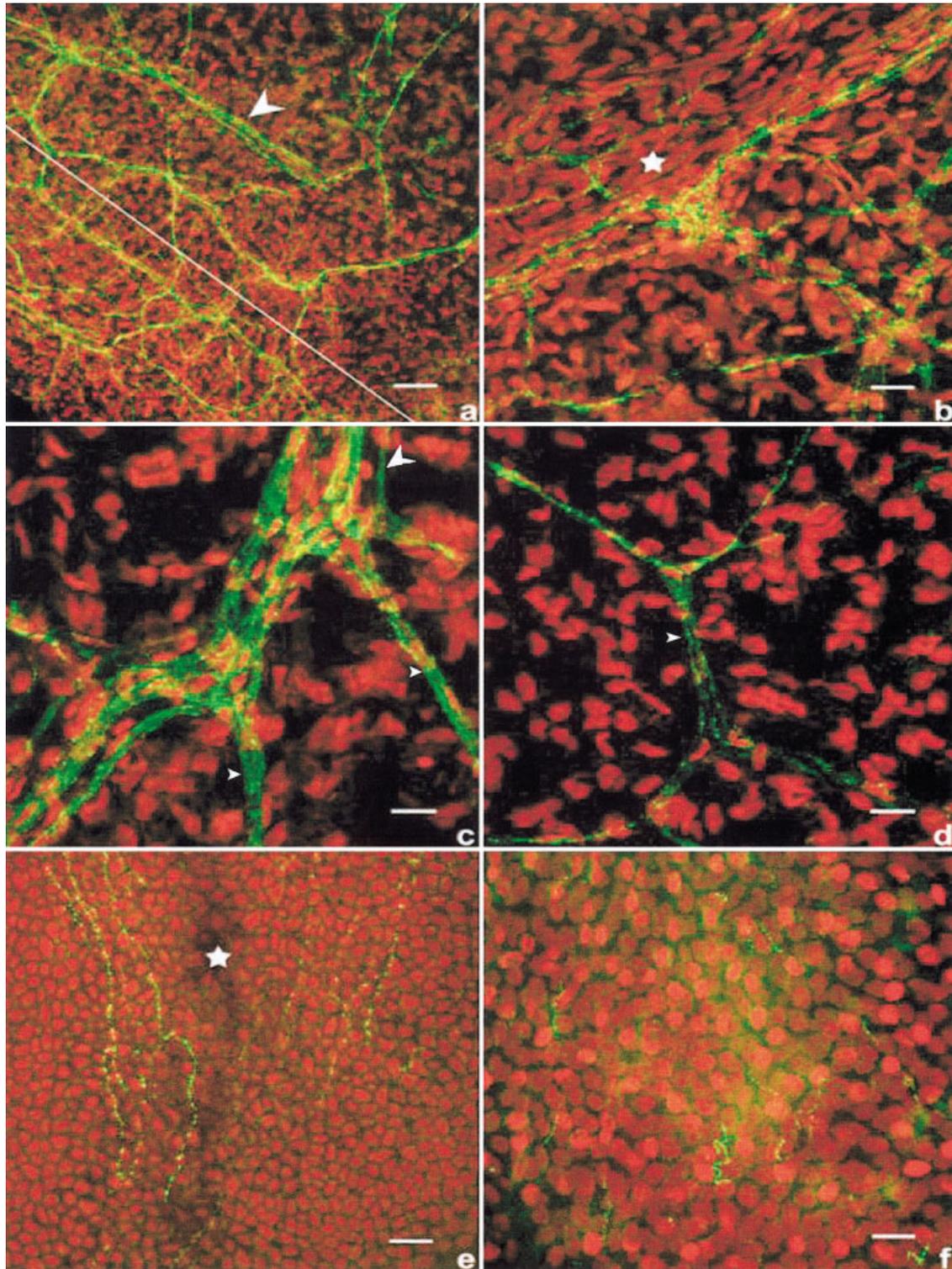
Fig. 3. Confocal scanning laser microscope Z-series images of WE-14 immunostaining of whole-mount preparation in the adult mouse limbo-corneal nerve net (green) with propidium iodide nuclear counter stain (red) (a–f). Each image represents a composite of CSLM Z series images generated from the following total section thickness; a, 9.1; b, 18.2; c, 3.2; d, 6.7; e, 17.0; f, 5.1 μm, respectively. Low-magnification image revealing the pattern of immunostaining in the limbo-corneal nerve net; the white line corresponds to the limbo-scleral junction with the major peripheral mid-stromal nerve fibre tracts that enter the cornea (arrowhead) from the limbus (**a**). Intense immunostaining in nerve fibres associated with unidentified superficial vessels (star) in the limbo-corneal junction (**b**). Varicose immunostaining localised to fibres in peripheral large mid-stromal fibre tracts (large arrowhead) and in minor fibre tracts passing toward (small arrowhead) (**c**), and forming the upper-stromal nerve tracts in the central cornea (small arrowhead) (**d**). A leash in the basal central corneal epithelium (Bowman's membrane: star) (**e**) and the corresponding (**f**) nerve fibres ramifying amongst squamous epithelium. Scale bar = (a) 50 μm, (b–f) 20 μm. [Color figure can be viewed in the online issue, which is available at www.interscience.wiley.com.]
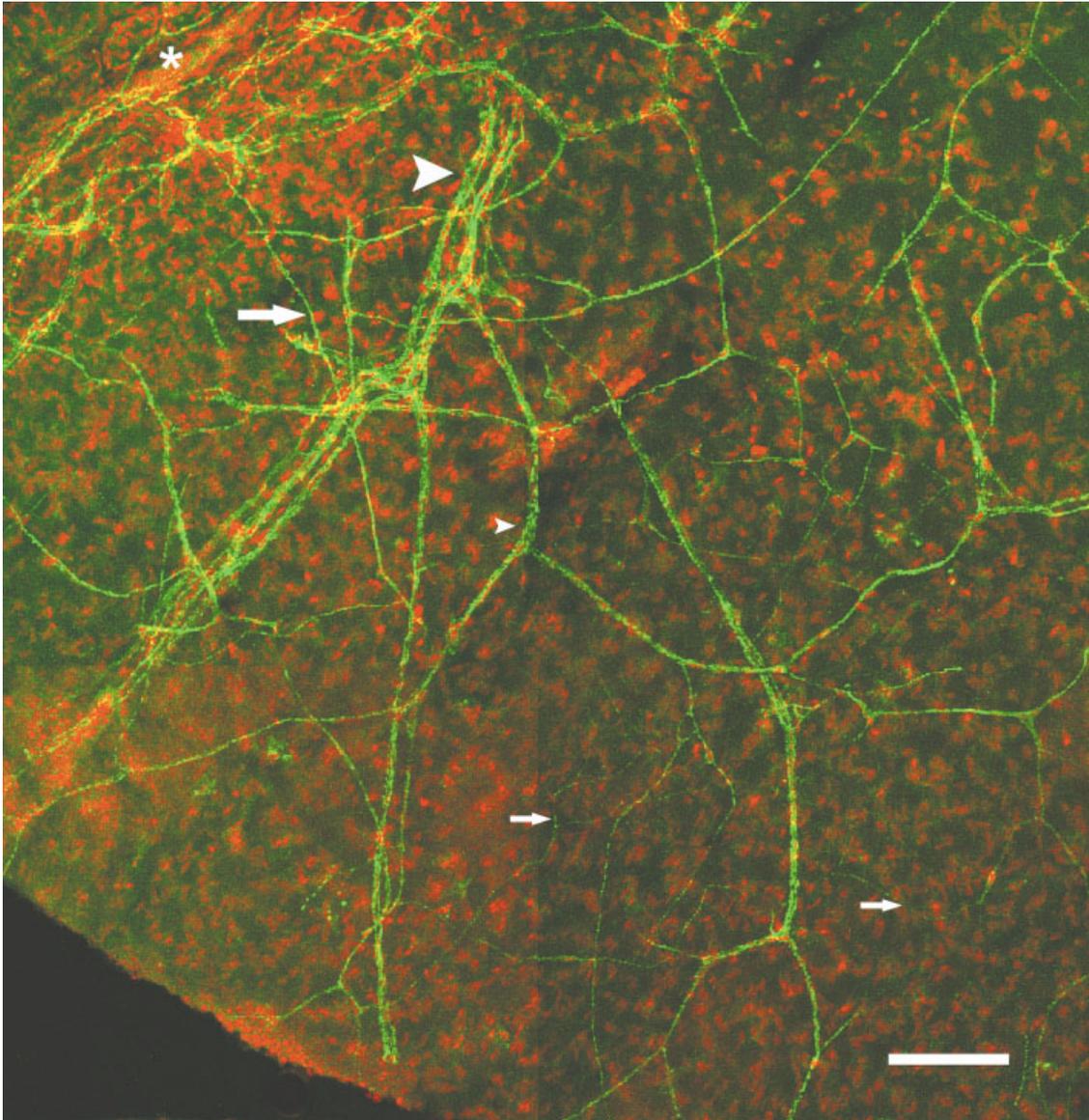
Fig. 4. A composite image of six contiguous confocal scanning laser microscope Z-series images of WE-14 immunostaining in a whole-mount preparation of adult mouse limbo-corneal nerve net (green) with propidium iodide nuclear counter stained (red). This image is representative of WE-14 immunostaining in a corneal segment (approximately one-eighth) in the mid to upper stromus from the limbo-corneal nerve net (star) to the central cornea adjacent to the scale bar (100 μm). The large fibre tracts that enter the mid-stromal region (large arrowhead) branch to form the upper stromal (small arrowhead) network, which gives rise to fine fibres (small arrows) that form leashes. A limited population of nerve fibres (large arrow) entered the peripheral cornea from the limbo-corneal network (star). (Mean section thickness 33.9 ± 8.3 μm). [Color figure can be viewed in the online issue, which is available at www.interscience.wiley.com.]

3a–f and 4). WE-14 immunostaining was evident in a sub-epithelial network of fibres in the limbo-corneal zone (Fig. 3a and b). Immunoreactivity was observed in peripheral prominent mid-stromal nerve fibre tracts that project toward the central cornea (Fig. 3c). Branches from these primary fibre tracts extend toward the upper stroma (Fig. 3c and d) forming a diffuse irregular network beneath Bruch's membrane (Fig. 3d); these latterly generate leashes in the basal epithelium (Fig. 3e). Individual varicose WE-14 immunopositive fibres were observed between the basal corneal epithelium and some of these nerve fibres terminated amongst the outer-most corneal epithelial cells (Fig. 3f). An overview of the pattern of mid to upper stromal WE-14 immunostaining in a tissue segment representing approximately a one-eighth area of cornea from the limbo-corneal junction to the central cornea was generated from six contiguous CLMS images (Fig. 4).

DISCUSSION

The complexity of peptidergic limbo-corneal innervation is evident, yet the biological role for these familiar

neuropeptides in this tissue is either inadequately defined or unknown (Marfurt, 2000). A previous study of adult porcine ocular tissue revealed that another neuropeptide WE-14 is generated in neuronal elements primarily within the anterior uvea and retina (Curry et al., 2003). This study of the developing mouse cornea has demonstrated that immunoreactivity for WE-14 was present in a subpopulation of fibres within the major mid-stromal and minor upper stromal nerve fibre tracts and in fine varicose fibres throughout the corneal epithelium. Several biological functions have been attributed to corneal neuropeptides; these include sensory perception and involvement in corneal epithelial regeneration. Additionally, the detection of neuropeptides adjacent to the limbal vasculature has led to the suggestion that they may be vasomodulators (Jones and Marfurt, 1998). The vasostatins represent candidate CgA-derived neuropeptides that may impact the local vasculature (Aardal and Helle, 1992). The distribution of WE-14 immunoreactivity observed in adult mouse limbo-cornea preparations was comparable to that of other neuropeptides. Therefore, it may exhibit comparable biological roles. However, the relatively sparse pattern of WE-14 immunostaining within fibre tracts relative to that reported for SP, NPY, CGRP, and galanin (Jones and Marfurt, 1998) would suggest that it is generated in a distinct type of neuron. The present study has not established if WE-14 or other CgA-derived peptides are generated in either sensory or autonomic nerves; determination of this parameter may offer some insight into their physiological role in corneal tissue.

Analysis of the developing rat cornea detected SP immunostaining at gestational day 17 (Sakiyama et al. 1984) and a dense CGRP corneal plexus was detected at birth (Jones and Marfurt, 1991). This contrasts with the weak diffuse WE-14 immunostaining detected in peripheral mid stromal nerve tracts in the mouse cornea at birth. A temporal pattern of WE-14 generation was detected in the developing rat neuroendocrine system. It was first observed in endocrine cells in the pancreas and stomach at E15.5, intestinal and chromaffin cells at E17.5, and in thyroid parafollicular cells at E18.5 (Barkatullah et al. 1997). The failure to detect WE-14 in neonatal limbo-corneal nerves would suggest that unlike SP and CGRP (Jones and Marfurt, 1991), it does not have a biological role in early corneal development.

The biological roles of diverse spectrum of neuropeptides in corneal pathophysiology are actively being sought. SP and CGRP receptors have been detected on limbal and corneal epithelial cells and increasing evidence suggests that some neuropeptides exhibit trophic functions (Heino et al. 1995; Kieselbach et al. 1990). Supporting evidence has been derived following capsaicin administration, which depletes corneal neuropeptide content, limiting corneal healing (Gallar et al. 1990). Studies thus far have revealed that WE-14 modulates mast cell histamine secretion (Forsythe et al. 1996). The detection of WE-14 in the cornea has further demonstrated the complexity of corneal innervation and studies are underway to assess the physiological role of WE-14 on corneal tissues.

REFERENCES

Aardal S, Helle KB. 1992. The vasoinhibitory activity of bovine chromogranin A fragment (vasostatin) and its independence of extracellular calcium in isolated segments of human blood vessels. Regul Pept 41:9–18.

Barkatullah SC, Curry WJ, Johnston CF, Hutton JC, Buchanan KD. 1997. Ontogenetic expression of chromogranin A and its derived peptides, WE-14 and pancreastatin in the rat neuroendocrine system. Histochem Cell Biol 107:251–258.

Barkatullah SC, Pogue KM, Depreitere J, Boutajangout A, Liang F, DePotter W, Curry WJ. 2001. Immunohistochemical localization of WE-14 in the developing porcine sympathoadrenal cell lineage. Histochem Cell Biol 116:255–262

Conlon JM, Hamberger B, Grimelius L. 1992 Isolation of peptides arising from the specific posttranslational processing of chromogranin A and chromogranin B from human pheochromocytoma tissue. Peptides 13:639–644.

Curry WJ, Johnston CF, Hutton JC, Arden SD, Rutherford NG, Shaw C, Buchanan KD. 1991. The tissue specific distribution of rat chromogranin A-derived peptides: evidence for differential tissue processing from sequence specific antisera. Histochem 96:532–538.

Curry WJ, Shaw C, Johnston CF, Thim L, Buchanan KD. 1992. Isolation and primary structure of a novel chromogranin A-derived peptide, WE-14, from a human midgut carcinoid tumour. FEBS Lett 301:319–321.

Curry WJ, Barkatullah S, Johansson AN, Quinn JG, Norlen P, Connolly CK, McCollum AP, McVicar CM. 2002. WE-14, a chromogranin A-derived neuropeptide. In: O'Connor DT, Eiden L, editors. The chromaffin cell: transmitter biosynthesis, storage, release, actions, and informatics. New York: ANYAS. p 311–316.

Curry WJ, McCollum AP, Brockbank S, Gardiner TA, Maule AG, Stitt AW. 2003. Characterisation of WE-14 in porcine ocular tissue. Regul Pept 113:41–47.

Forsythe P, Curry WJ, Johnston CF, Harriott P, MacMahon J, Ennis M. 1996. The modulatory effects of WE-14 on histamine release from rat peritoneal mast cells. Inflamm Res 64:S13–S16

Gallar J, Pozo MA, Rebollo I, Belmonte C. 1990. Effects of capsaicin on corneal wound healing. Invest Ophthalmol Vis Sci 31:1968–1974.

Gasparri A, Sidoli A, Sanchez LP, Longhi R, Siccardi AG, Marchisio PC, Corti A. 1997. Chromogranin A fragments modulate cell adhesion. Identification and characterization of a pro-adhesive domain. J Biol Chem 272:20835–20843.

Gleeson CM, Curry WJ, Johnston CF, Buchanan KD. 1996. Occurrence of WE-14 and chromogranin A derived peptides in tissues of the human and bovine gastro-entero pancreatic system and in human neuroendocrine neoplasia. J Endocrinol 151:409–420.

Gibson CJ, Munoz DG, 1993 Chromogranin A inhibits retinal dopamine release. Brain Res 622:303–306

Gorr SU, Shioi J, Cohn DV. 1989. Interaction of calcium with porcine adrenal chromogranin A (secretory protein-I) and chromogranin B (secretogranin I). Am J Physiol 257:E247–E254.

Heaney AP, Curry WJ, Pogue KM, Armstrong VL, Mirakhur M, Sheridan B, Johnston CF, Buchanan KD, Atkinson AB. 2000. Immunohistochemical evaluation of the post-translational processing of chromogranin A in human pituitary adenomas. Pituitary 3:67–75.

Heino P, Oksala O, Luhtala J, Uusitalo H. 1995. Localization of calcitonin gene-related peptide binding sites in the eye of different species. Curr Eye Res 14:783–790.

Helle KB. 2000. The chromogranins. Historical perspectives. Adv Exp Med Biol 482:3–20.

Hutton JC, Nielsen E, Kastern W. 1988. The molecular cloning of the chromogranin A-like precursor of beta-granin and pancreastatin from the endocrine pancreas. FEBS Lett 236:269–274.

Jones MA, Marfurt CF. 1991. Calcitonin gene-related peptide and corneal innervation: a developmental study in the rat. J Comp Neurol. 313:132–150.

Jones MA, Marfurt CF. 1998. Peptidergic innervation of the rat cornea. Exp Eye Res 66:421–435.

Kieselbach GF, Ragaut R, Knaus HG, Konig P, Wiedermann CJ. 1990. Autoradiographic analysis of binding sites for 125I-Bolton-Hunter-substance P in the human eye. Peptides 11:655–659.

Kirchmair R, Benzer A, Troger J, Miller C, Marksteiner J, Saria A, Gasser RW, Hogue-Angeletti R, Fischer-Colbrie R, Winkler H. 1994. Molecular characterization of immunoreactivities of peptides derived from chromogranin A (GE-25) and from secretogranin II (secretoneurin) in human and bovine cerebrospinal fluid. Neuroscience 63:1179–1187.

Lugardon K, Raffner R, Goumon Y, Corti A, Delmas A, Bulet P, Aunis D, Metz-Boutigue MH. 2000. Antibacterial and antifungal activities

of vasostatin-1, the N-terminal fragment of chromogranin A. 275: 10745–10753.

Mahata SK, O'Connor DT, Mahata M, Yoo SH, Taupenot L, Wu H, Gill BM, Parmer RJ. 1997. Novel autocrine feedback control of catecholamine release. A discrete chromogranin a fragment is a noncompetitive nicotinic cholinergic antagonist. J Clin Invest 100: 1623–1633.

Marfurt CF. 2000. Nervous control of the cornea. In: Burnstock G, Sillito AM, editors. Nervous control of the eye. Amsterdam: Harwood Academic Publishers. p 41–92.

Marfurt CF, Ellis LC, Jones MA. 1993. Sensory and sympathetic nerve sprouting in the rat cornea following neonatal administration of capsaicin. Somatosens Mot Res 10:377–398.

Miller A, Costa M, Furness JB, Chubb IW. 1981. Substance P immunoreactive sensory nerves supply the rat iris and cornea. Neurosci Lett 23:243–249.

Moller K, Zhang YZ, Hakanson R, Luts A, Sjolund B, Uddman R, Sundler F. 1993. Pituitary adenylate cyclase activating peptide is a sensory neuropeptide: immunocytochemical and immunochemical evidence. Neuroscience 57:725–732.

Nolan JA, Trojanowski JQ, Hogue-Angeletti R. 1985. Neurons and neuroendocrine cells contain chromogranin: detection of the molecule in normal bovine tissues by immunochemical and immunohistochemical methods. J Histochem Cytochem 33:791–798.

Norlen P, Curry WJ, Bjorkquvist M, Maule A, Cunningham RT, Hogg RB, Harriott P, Johnston CF, Hutton JC, Hakanson R. 2001. Cell-specific processing of chromogranin A in endocrine cells of the rat stomach. J Histochem Cytochem 49:9–18

Palkama A, Uusitalo U, Lehtosalo J. 1986. Innervation of the anterior segment of the eye: with special reference to functional aspects. In: Panula P, Aaivarienta H, Soinila S, editors. Neurohistochemistry: modern methods and applications. New York: Alan R. Liss. p 587–615

Reiffen FU, Gratzl M. 1986. Chromogranins, widespread in endocrine and nervous tissue, bind Ca^{2+}. FEBS Lett 195:327–330.

Sakiyama T, Kuwayama Y, Ishimoto I, Sasaoka A, Shiosaka S, Tohyama M, Manabe R, Shiotani Y. 1984. Ontogeny of substance P-containing structures in the ocular tissue of the rat: an immunohistochemical analysis. Brain Res 315:275–281.

Stone RA, McGlinn AM. 1988a. Calcitonin gene-related peptide immunoreactive nerves in human and rhesus monkey eyes. Invest Ophthalmol Vis Sci 29:305–310.

Stone RA, McGlinn AM, Kuwayama Y. 1988b. Galanin-like immunoreactive nerves in the porcine eye. Exp Eye Res 46:457–461.

Tatemoto K, Efendic S, Mutt V, Makk G, Feistner GJ, Barchas JD. 1986. Pancreastatin, a novel pancreatic peptide that inhibits insulin secretion. Nature 324:476–478.

Tinsley PW, Fridland GH, Killmar JT, Desiderio DM. 1988. Purification, characterization, and localization of neuropeptides in the cornea. Peptides 9:1373–1379.

Too HP, Todd K, Lightman SL, Horn A, Unger WG, Hanley MR. 1989. Presence and actions of vasopressin-like peptides in the rabbit anterior uvea. Regul Pept 25:259–266.

Ueda S, del Cerro M, LoCascio JA, Aquavella JV. 1989. Peptidergic and catecholaminergic fibers in the human corneal epithelium. An immunohistochemical and electron microscopic study. Acta Ophthalmol Suppl 192:80–90.

Yamamoto R, McGlinn A, Stone RA. 1991. Brain natriuretic peptide-immunoreactive nerves in the porcine eye. Neurosci Lett 122:151–153.

Zander E, Weddell G. 1951. Observations of the innervation of the cornea. J Anat 85:68–99.